Room temperature midinfrared electroluminescence from InAs quantum dots

D. Wasserman,[1,a)] T. Ribaudo,[1] S. A. Lyon,[2] S. K. Lyo,[3] and E. A. Shaner[3]
[1]*Department of Physics, University of Massachusetts Lowell, Lowell, Massachusetts 01854, USA*
[2]*Department of Electrical Engineering, Princeton University, Princeton, New Jersey 08544, USA*
[3]*Sandia National Laboratories, P.O. Box 5800, Albuquerque, New Mexico 87185, USA*

(Received 16 January 2009; accepted 22 January 2009; published online 9 February 2009)

We demonstrate room temperature midinfrared electroluminescence from intersublevel transitions in self-assembled InAs quantum dots. The dots are grown in GaAs/AlGaAs heterostructures designed to maximize current injection into dot excited states while preferentially removing electrons from the ground states. As such, these devices resemble quantum cascade lasers. However, rigorous modeling of carrier transport through the devices indicates that the current transport mechanism for quantum dot active regions differs from that of quantum-well-based midinfrared lasers. We present the calculated energy states and transport mechanism for an intersublevel quantum dot emitter, as well as experimental electroluminescence data for these structures. © *2009 American Institute of Physics*. [DOI: 10.1063/1.3080688]

The rapid development of the quantum cascade laser (QCL)[1] has provided high power semiconductor light sources across a wide range of midinfrared (mid-IR) and terahertz frequencies,[2–5] utilizing optical transitions between conduction band states in multiple periods of complex heterostructures. Because QCLs are effectively collections of quantum wells (QWs), the two-dimensional active region density of states provides numerous scattering paths for electrons relaxing from the upper to lower laser states, leading to ultrafast nonradiative relaxation times (approximately picosecond). This allows for high speed modulation of QC lasers and high slope efficiencies once the laser reaches threshold (J_{th}), though it also results in high J_{th}'s, limiting the wall plug efficiency of QCLs. In addition, because the optical transitions are between states confined in the growth direction, QCLs emit light polarized in the growth direction and are usually fabricated in ridge waveguide structures. Surface emission from such devices requires fabrication-intensive and wavelength specific surface output couplers.[6]

There is thus significant interest in both improved efficiency for mid-IR semiconductor emitters, as well as naturally surface emitting devices. The use of quantum boxes, or three-dimensional (3D) nanostructures, in the active regions of quantum cascadelike devices offers a path toward the development of higher efficiency, surface emitting mid-IR sources. The increased quantization of the electrons in these nanostructures changes the density of states in the laser active region to atomlike delta functions, making nonradiative recombination between electron states more difficult (the so-called "phonon bottleneck").[7] As an example of this effect, it has been shown that QCLs placed in a magnetic field perpendicular to the growth plane exhibit, at certain fields, significant increases in efficiency due to the additional quantization from the formation of Landau levels.[8]

An alternative method for the 3D quantization of states in mid-IR emitters is the incorporation of self-assembled quantum dots (SAQDs). Such QDs can be grown by molecular beam epitaxy (MBE) using the Stranski–Krastanow[9] growth process. Under the right growth conditions, these SAQDs form with minimal defects, making them prime candidates for a multitude of optical and electronic applications. Although there remains some debate over the nonradiative relaxation time for electrons in SAQD excited states, most experimental results demonstrate times orders of magnitude longer than in QW structures,[10–13] indicating the feasibility of QD-based mid-IR emitters.

Research into the mid-IR properties of QDs, mostly for photodetector applications, has been ongoing for some time.[14–16] Early mid-IR emission from InAs QDs, never definitively resulting in lasing, was seen from devices designed for interband, near-IR lasing.[17,18] In later work, unipolar devices employing cascadelike heterostructure designs demonstrated mid-IR electroluminescence (EL), though emission was weak and limited to low temperatures.[19,20]

Some of the challenges facing the development of QD mid-IR sources come from the effort to design such structures along the lines of QCLs. QCL development has progressed at its breakneck pace in part because of researchers' ability to design and accurately model the lasers they are studying. The incorporation of QDs into the QC active region makes modeling of such structures far more difficult even if QDs grew with uniform and controllable sizes and shapes. Unfortunately, SAQDs do not necessarily grow uniformly or ordered (Fig. 1 inset), making predictions of device performance very challenging.

Recently, we have made significant progress in the modeling, design, and subsequent growth and fabrication of mid-IR QD emitters. All of our samples are grown by MBE on highly *n*-doped GaAs substrates. As shown in Fig. 1, we use a graded AlGaAs injector to inject electrons into QD excited (*p*) states. A thin (30/11 Å) AlGaAs/AlAs barrier separates the AlGaAs injector from the dot layer. This layer serves as an injection barrier and is designed to provide additional quantum confinement to the QD states in order to increase the ground (*s*) state energy in the dots above the GaAs bandedge. Pushing the QD ground states above the GaAs bandedge is essential for effective extraction of carriers from the QDs. The InAs layer deposition was terminated

a)Electronic mail: daniel_wasserman@uml.edu.

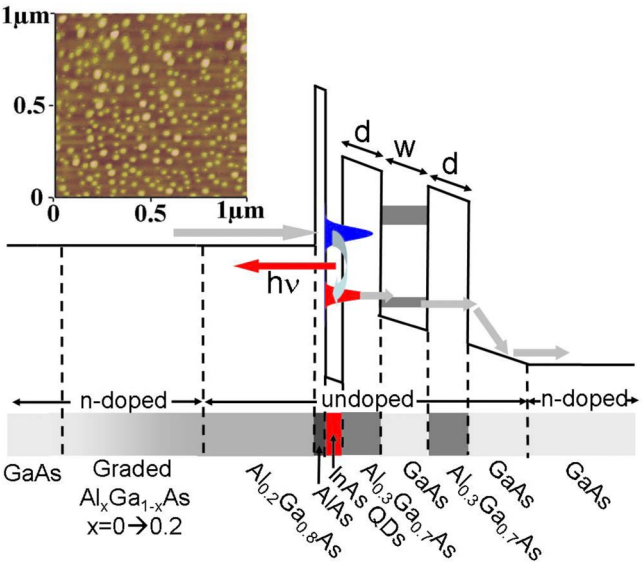

FIG. 1. (Color online) Conduction band diagram for biased QD mid-IR emitters studied in this work. Electrons are injected into QD excited states via a graded AlGaAs injector. Extraction from the lower dot states (and confinement to upper dot states) is achieved by means of a downstream QW filter. Electron flow is from left to right; energies are not to scale. Inset shows AFM image of InAs QD layer.

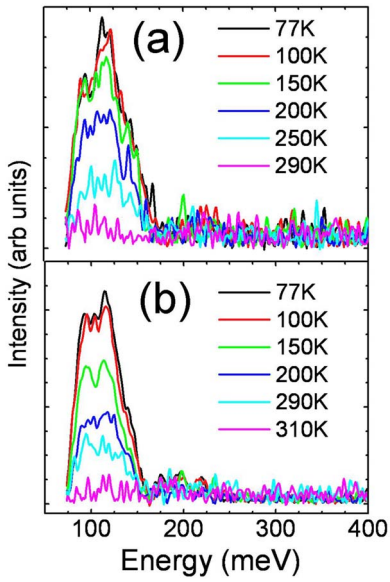

FIG. 2. (Color online) Temperature dependent electroluminescence spectra for (a) mm199 and (b) mm290, which emit at temperatures as high as 290 K.

immediately upon formation of the QD structures, so as to maintain a small QD size and thus high energy QD ground states. A QW filter on the downstream side of the QD layer prevents electron tunneling directly through the QD layer and forces an optical transition in the QD. Electrons are then extracted from the ground state of the QD via the ground state of the QW filter.

Two samples were grown with slightly different device structures. The basic design of each device, shown in Fig. 1, consisted of the ramped AlGaAs injector and thin AlAs tunnel barrier, followed by the QD layer and a downstream QW structure. In sample mm199, the QW consisted of a 23 Å $Al_{0.3}Ga_{0.7}As$ barrier, followed by a 51 Å GaAs well and a 23 Å $Al_{0.35}Ga_{0.65}As$ barrier. Sample mm290 differed from sample mm199 only in the QW design, consisting of an 80 Å $Al_{0.3}Ga_{0.7}As$ barrier, followed by a 60 Å GaAs well and a second 80 Å $Al_{0.3}Ga_{0.7}As$ barrier.

Devices were fabricated by deposition and annealing of large-aperture Ohmic *n*-GaAs contacts designed for surface emitting devices. Electroluminescence of the samples was measured on a Bruker V70 Fourier transform IR spectrometer operating in amplitude modulation step-scan mode. Samples were mounted in a liquid-nitrogen-cooled cryostat, and spectra were collected as a function of temperature for pulsed operation at 40 kHz repetition rates and 40% duty cycle. In addition, emission spectra were measured as a function of applied voltage, modulation frequency, and pulse duty cycle, though no changes in the spectral shape were observed for variations in these parameters.

Figure 2 shows the devices' temperature dependent electroluminescence spectra. Clear emission spectra, peaking at approximately 120 meV (10.3 μm), was seen at low temperatures for each sample. The emission shows a clear decrease in intensity as a function of temperature. This decrease in emission power, for a constant voltage, can be attributed to the thermionic emission of electrons from the upper state of the QDs, leading to leakage current. However, the thicker QW barriers of sample mm290 increase the confinement of electrons in the QD *p*-states, which in turn leads to lower thermionic emission at elevated temperatures and thus room temperature emission. In addition, mm290 outperformed mm199 at low temperatures (80 K), with emission intensities of approximately a factor of three stronger than that of mm199.

The low-temperature (77 K) current-voltage (*I-V*) curve for sample mm290 shows a current turn-on at approximately 1.5 V, corresponding to the flattening of the graded AlGaAs injector barrier and thus efficient current injection into the device structure. The *I-V* curve for sample mm290 can be compared to the EL intensity as a function of applied bias for a light-emitting device. The emitter shows no luminescence for voltages below 0.6 V, and the emission intensity increases linearly up to 3 V, at which point the emission begins to saturate. No spectra were taken above 3.5 V in order to prevent voltage breakdown of the sample.

The low-temperature electronic structure of, and current transport through, our devices was developed using the COMSOL MULTIPHYSICS package. Efficient electron injection into the active region occurs when the conduction band edge of the graded region is aligned with that of the $Al_{0.2}Ga_{0.8}As$ layer in Fig. 1 and the Fermi sea comes in contact with this layer. The steep linear increase in the current at 1.5 V in Fig. 3 indicates that both alignment and energy conservation conditions are satisfied near $\sim$1.5 V. The tunneling current increases as more *p*-levels in the distribution fall into the resonance band and as the tunneling barrier decreases with increasing bias. The small current in Fig. 3 below 1.5 V may be due to activated tunneling. At alignment, the Fermi energy is roughly $E_F \sim 8$ meV. At 0 V, our numerical estimate gives $E_p = 12$ meV and $E_s = -96$ meV with $E=0$ at the conduction band edge of the $Al_{0.2}Ga_{0.8}As$ layer. These levels will be somewhat lower at the alignment bias. The electroluminescence data in Fig. 2 indicate that there is a width of about 50 meV of *p*- and *s*-levels due to dot size fluctuation. As bias is increased, tunneling starts as the low-energy tail of the *p*-level distribution falls into the energy resonance band

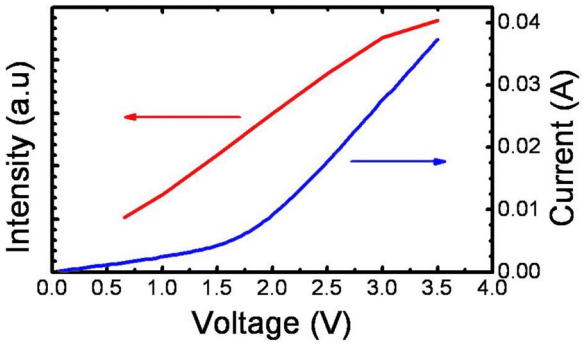

FIG. 3. (Color online) Low-temperature (77 K) light intensity vs voltage (red) and current vs voltage (blue) plots for sample mm290.

between $E=0$ and E_F for energy conservation $0 \leq E_p = E(k_z) + E(k_\perp) \leq E_F$, where $E(k_\alpha) = \hbar^2 k_\alpha^2 / 2m^*$ and $k_\perp^2 = k_x^2 + k_y^2$. The tunneling probability becomes small for a large $E(k_\perp)$ when the overlap of the plane waves in the x, y directions with the QD is small due to spatial oscillations for $k_\perp L_{QD} \gg 1$. Here L_{QD} is the QD size in these lateral directions.

The second level of the GaAs QW lies about 34 meV above the *p*-level at zero bias. Our goal is to keep this QW level above the *p*-level of the biased QD and use energy conservation to inhibit tunneling between these two levels, forcing radiative transitions from the *p*- to *s*-levels. Tunneling from the *p*-level to the ground QW ground state (which is about 125 meV below the QD *p*-state energy at zero bias) is negligible because this large energy difference has to be dissipated into the in-plane kinetic energy with $k_\perp L_{QD} \gg 1$. However, the ground QW level is about 18 meV below the *s*-level at zero bias, and rapid tunneling is allowed between these two levels. There are uncertainties in the relative energy differences between these levels at a finite bias in the presence of the QD size fluctuations. The light intensity in Fig. 3 begins to saturate above 3.0 V, indicating that the second level of the QW falls below the *p*-levels, allowing an additional current leakage channel.

At higher temperatures, electrons in the *p*-state of the QDs are activated to higher intradot levels and make nonradiative tunneling transitions to the second level of the QW, bypassing the *s*-state. The leakage can also occur through direct phonon-assisted tunneling from the *p*-state to the second level of the QW. Both processes result in decreased emission intensity, though a quantitative prediction of the decreased efficiency would require a better understanding of the nature of the higher QD states and is beyond the scope of the current work.

In summary, mid-IR emitters were designed for optimization of intersublevel optical transitions between states confined in InAs SAQDs. Careful modeling and design of our devices resulted in electroluminescence up to room temperature. The ability to efficiently inject and extract electrons from the appropriate energy levels in mid-IR QD emitters is an important step toward the development of a class of mid-IR light sources based on intersublevel transitions in 3D quantum nanostructures. We demonstrate here the ability to model and grow such structures and clearly show the improved device performance achievable with such a comprehensive approach.

Sandia is a multiprogram laboratory operated by Sandia Corporation, a Lockheed Martin Co., for the United States Department of Energy's National Nuclear Security Administration under Contract No. DE-AC04-94AL85000.

[1] J. Faist, F. Capasso, D. L. Sivco, C. Sirtori, A. L. Hutchinson, and A. Y. Cho, Science **264**, 553 (1994).
[2] L. Diehl, D. Bour, S. Corzine, J. Zhu, G. Höfler, M. Lončar, M. Troccoli, and F. Capasso, Appl. Phys. Lett. **88**, 201115 (2006).
[3] A. Lyakh, P. Zory, D. Wasserman, G. Shu, C. Gmachl, M. D'Souza, D. Botez, and D. Bour, Appl. Phys. Lett. **90**, 141107 (2007).
[4] Y. Bai, S. R. Darvish, S. Slivken, W. Zhang, A. Evans, J. Nguyen, and M. Razeghi, Appl. Phys. Lett. **92**, 101105 (2008).
[5] R. Köhler, A. Tredicucci, F. Beltram, H. E. Beere, E. Linfield, A. G. Davies, D. A. Ritchie, R. C. Iotti, and F. Rossi, Nature (London) **417**, 156 (2002).
[6] R. Colombelli, K. Srinivasan, M. Troccoli, O. Painter, C. Gmachl, D. M. Tennant, A. M. Sergent, D. L. Sivco, A. Y. Cho, and F. Capasso, Science **302**, 1374 (2003).
[7] H. Benisty, C. M. Sotomayor-Torres, and C. Weisbuch, Phys. Rev. B **44**, 10945 (1991).
[8] D. Smirnov, C. Becker, O. Drachenko, V. V. Ryklov, H. Page, J. Leotin, and C. Sirtori, Phys. Rev. B **66**, 121305 (2002).
[9] N. Stranski and L. Krastanow, Sitzungsber. Akad. Wiss. Wien, Math.-Naturwiss. Kl., Abt. 2B **146**, 797 (1938).
[10] P. D. Buckle, P. Dawson, S. A. Hall, X. Chen, M. J. Steer, D. J. Mowbray, M. S. Skolnick, and M. Hopkinson, J. Appl. Phys. **86**, 2555 (1999).
[11] L. Zhang, T. F. Boggess, K. Gundogdu, M. E. Flatte, D. G. Deppe, C. Cao, and O. B. Shchekin, Appl. Phys. Lett. **79**, 3320 (2001).
[12] R. Heitz, H. Born, F. Guffarth, O. Stier, A. Schliwa, A. Hoffmann, and D. Bimberg, Phys. Rev. B **64**, 241305 (2001).
[13] E. W. Bogaart, J. E. M. Haverkort, T. Mano, T. van Lippen, R. Notzel, and J. H. Wolter, Phys. Rev. B **72**, 195301 (2005).
[14] K. W. Berryman, S. A. Lyon, and M. Segev, J. Vac. Sci. Technol. B **15**, 1045 (1997).
[15] D. Pan, E. Towe, and S. Kennerly, Appl. Phys. Lett. **73**, 1937 (1998).
[16] W. Zhang, H. Lim, M. Taguchi, S. Tsao, B. Movaghar, and M. Razeghi, Appl. Phys. Lett. **86**, 191103 (2005).
[17] L. E. Vorob'ev, D. A. Firsov, V. A. Shalygin, V. N. Tulupenko, Y. M. Shernyakov, N. N. Ledentsov, V. M. Ustinov, and Zh. I. Alferov, JETP Lett. **67**, 275 (1998).
[18] S. Krishna, P. Bhattacharya, P. J. McCann, and K. Nanjou, Electron. Lett. **36**, 1550 (2000).
[19] D. Wasserman and S. A. Lyon, Appl. Phys. Lett. **81**, 2848 (2002).
[20] S. Anders, L. Rebohle, F. F. Schrey, W. Schrenk, K. Unterrainer, and G. Strasser, Appl. Phys. Lett. **82**, 3862 (2003).